Wear 310 (2014) 51–62

Contents lists available at ScienceDirect

Wear

journal homepage: www.elsevier.com/locate/wear

Effects of sigma phase and carbide on the wear behavior of CoCrMo alloys in Hanks′ solution

Yan Chen [a], Yunping Li [b,*], Shingo Kurosu [b], Kenta Yamanaka [a], Ning Tang [b], Yuichiro Koizumi [b], Akihiko Chiba [b,**]

[a] Tohoku University, Department of Material Science and Engineering, Sendai 980-8579, Japan
[b] Institute for Material Research, Sendai 980-8577, Japan

ARTICLE INFO

Article history:
Received 9 September 2013
Received in revised form
6 December 2013
Accepted 11 December 2013
Available online 19 December 2013

Keywords:
CoCrMo alloy
σ phase
Carbide
Wear behavior
Contact mechanics
Surface fatigue

ABSTRACT

This study aims to elucidate the synergy effects of the σ phase and carbide on the wear behavior of low-carbon (LC) and high-carbon (HC) cobalt–chromium–molybdenum (CoCrMo) alloys, by using pin-on-disc tests under Hanks′ lubricated conditions. Fractured or torn-off σ-phase precipitates were observed to be the main reason for abrasion for both LC and HC alloys. Carbides were torn off at the initial high contact pressure to form pitting; σ-phase precipitates around the pitting were uprooted and led to micro cracks, which is considered as surface fatigue of HC alloy. In contrast, strain-induced martensite observed on the worn surface was contributed to the increase of hardness and abrasion resistance of LC alloy.

1. Introduction

Cobalt–chromium–molybdenum (CoCrMo) alloys have been widely used in gas turbines, dental and orthopedic implants [1–5], as the group of cobalt-base alloys can be commonly described as wear, corrosion and heat resistant [6]. Up to now, the largest use of wear resistant components and/or their applications appeal for persistent and further studies of CoCrMo alloy.

Properties of CoCrMo alloys can be improved by change of cobalt crystallographic nature, solid-solution-strengthening effect of alloying elements (Cr, Mo, W et al.), and formation of second phase such as carbides [7]. However, the alloys′ compositions of today are little changed from the early ones of Elwood Haynes but for tremendous amount and type of carbide formation in the microstructure [6]. Therefore, plenty of researches focusing on how carbides affect the wear behavior of the CoCrMo alloy have been conducted. Fulcher et al. [8] and Desai et al. [9] found that the abrasive wear resistance increased monotonically with increasing volume fraction and size of the carbide phase, respectively, for a series of CoCr alloys. Cawley et al. [10] also reported that the as-cast CoCrMo alloy containing the highest volume fraction of blocky carbide showed the lowest wear rate. Similar conclusions were drawn by Scholes and Unsworth [11] and Tipper et al. [12], who suggested that the improved hardness and wear resistance could be attributed to the presence of carbides in wrought CoCrMo alloys. However, the opposite viewpoint that the hard precipitate phases (e.g., $M_{23}C_6$-type carbides) are detrimental to the wear behavior was also espoused by Wimmer et al. [13] and Chiba et al. [14], because hard carbide is prone to being torn off from the rubbing surfaces, resulting in three-body abrasive wear. It could be concluded that the type, distribution, morphology and volume fraction of carbide have significant influence to wear resistance for various CoCrMo alloys.

In the typical carbon- and nitrogen-containing CoCrMo alloy system, the precipitation of carbide and σ phases is unavoidable since most hot working and heat treatments are carried out below ~1373 K [15,16]. However, no detailed observation on interaction between the carbide and σ phases on the wear behaviors of these alloys has been identified so far. Therefore, the aim of the present study is to elucidate the synergy effects of the σ phase and carbide on the wear behavior of CoCrMo alloys by performing pin-on-disc wear tests in Hanks′ lubricated environment.

2. Experimental procedure

2.1. Materials

The materials used in this study are low-carbon (LC) and high-carbon (HC) Co–28Cr–6Mo alloys, with the compositions listed in

* Corresponding author. Tel.: +81 22 215 2452; fax: +81 22 215 2116.
** Corresponding author. Tel.: +81 22 215 2115; fax: +81 22 215 2116.
E-mail addresses: chenyan@imr.tohoku.ac.jp (Y. Chen), lyping@imr.tohoku.ac.jp, yunpinglee@gmail.com (Y. Li), kurosu@imr.tohoku.ac.jp (S. Kurosu), k_yamanaka@imr.tohoku.ac.jp (K. Yamanaka), ningtang@imr.tohoku.ac.jp (N. Tang), koizumi@imr.tohoku.ac.jp (Y. Koizumi), a.chiba@imr.tohoku.ac.jp (A. Chiba).

0043-1648/$ - see front matter Crown Copyright © 2013 Published by Elsevier B.V. All rights reserved.
http://dx.doi.org/10.1016/j.wear.2013.12.010

Table 1
Chemical compositions of LC and HC alloys (wt%).

Ingots	Co	Cr	Mo	C	Si	Mn	N
LC	Bal.	27.7	5.5	0.05	0.52	0.55	0.13
HC	Bal.	27.6	5.5	0.27	0.65	0.57	0.14

Table 1. Hot forging process for the ingots were: (1) vacuum induction melting process; (2) heating to 1523 K at a heating rate of 1 K/s with a homogenization holding for 18 h, followed by air cooling; (3) hot forging at 1273 K with a total reduction of ~45%; and (4) water quenching. The mechanical properties were evaluated in hardness tests (Shimadzu, HMV) and Young's modulus measurements, and the densities were evaluated using the Archimedes method.

2.2. Microstructure characterization

Pins and discs were machined to dimensions of ϕ 6 mm × 20 mm and ϕ 30 mm × 5 mm, respectively. The spherical contact ends of the pins (*SR* 2.4 mm) were ground with emery paper of up to #6000 grit and polished with a silica suspension. The discs were prepared with a sequence of polishing with 180–1200 grit emery papers, 30-min polishing with alumina and silica suspensions, and finally electropolishing in an electrolyte (methanol:sulfuric acid = 9:1) at 6 V, room temperature. The microstructure of disc surface was observed by performing scanning electron microscopy (SEM, Hitachi S3400N), electron probe microanalysis (EPMA, JXA-8530F, JEOL) and transmission electron microscope (TEM, JEM-2000EX II). The phase constitution of the matrix was identified by performing X-ray diffraction (XRD, Philips X' Pert) measurements with Cu *K*α radiation over $40^\circ < 2\theta < 55^\circ$, focused on three locations on each disc. Elaborate XRD measurements were performed using the monochrome model over $35^\circ < 2\theta < 55^\circ$ to determine the second phase precipitates.

2.3. Pin-on-disc test

All the specimens were ultrasonically cleaned with distilled water and ethanol (Kaijo sonocleaner 200D), then dried for 21.6 ks at room temperature in an air atmosphere in advance. The pin-on-disc test was conducted using a RHSCA FRP-2000 tribometer, as shown schematically in Fig. 1. The pin was mounted with a 9.8 N load representing a harsh contact (initial contact pressure: 1.69 GPa) [17], and tested against a disc rotating at 20 mm/s (24 rpm). The temperature was set to 37 ± 2 °C in an argon atmosphere, and the rotation radius was 8 mm. The lubricant was Hanks' solution, with its composition listed in Table 2. The test was performed over a continuous period of 60.48 ks for a total sliding distance of ~12.1 km. All tests were repeated 3 times for both LC and HC alloys.

The worn specimens were cleaned ultrasonically in distilled water and ethanol, and then dried for weight loss measurement using a direct-reading balance (Shimadzu AUW 320). The wear factor was calculated according to the most frequently used equation [18]

$$\omega_s = M_{loss}/(w \times s \times \rho) \quad (1)$$

where M_{loss} is weight loss, w is the normal load, s is the sliding distance, and ρ is the density of the specimen. The worn surfaces were analyzed using XRD, SEM and laser microscope (LM, Keyence KV-x200 series). The phase volume fractions were quantitatively

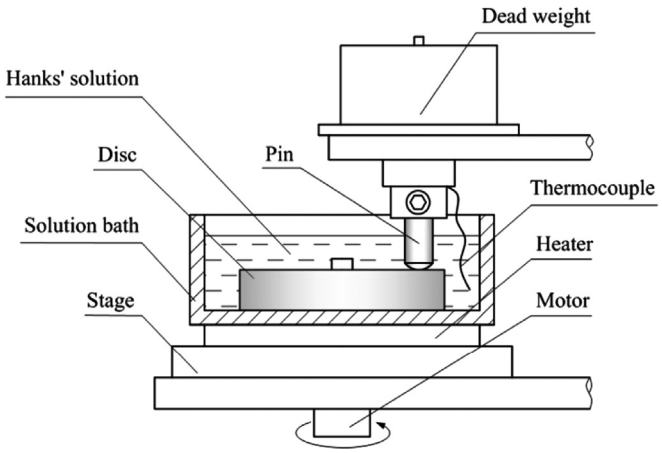

Fig. 1. Schematic diagram showing the basic working principle of the pin-on-disc test.

Table 2
Chemical composition of Hanks' solution (g/L).

NaCl	KCl	$CaCl_2$	$NaHCO_3$	$Na_2HPO_4 \cdot 2H_2O$	KH_2PO_4	$MgSO_4 \cdot 7H_2O$
8.0	0.4	0.14	0.35	0.06	0.06	0.2

Table 3
Basic properties of LC and HC alloys.

	LC	HC
Density (g/cm^3)	8.4	8.3
Young's modulus (GPa)	220	220
Vickers hardness, HV1	420	447

calculated according to Eq. (2), as proposed by Sage and Guillaud [19]

$$\frac{x}{1-x} = \frac{1}{4} \times \frac{1.85}{0.27} \times \frac{I_{(2\ 0\ 0)\gamma}}{I_{(1\ 0\ \bar{1}\ 1)\varepsilon}} \quad (2)$$

where x is the volume fraction of the face cubic centered γ phase and $I_{(2\ 0\ 0)\gamma}$ and $I_{(1\ 0\ \bar{1}\ 1)\varepsilon}$ are the integrated intensities of the (2 0 0)γ and (1 0 $\bar{1}$ 1)ε peaks, respectively.

The cross section of the worn surface was cut by a focused ion beam (FIB, QUANTA 200 3D, FEI) and observed using TEM. The hardness and roughness of as-polished and worn surfaces were evaluated with a Vickers hardness tester (Shimazu, HMV), a stylus profilometer (Surfcorder DSF 500) and LM, respectively. The wear debris was isolated from the Hanks' solution by Omnipore membrane filter paper (Millipore 0.2 μm JG, Ireland), then dispersed ultrasonically in ethanol for 30 min for SEM observation.

3. Results

3.1. Material characterization

The properties of the alloys are tabulated in Table 3. Both LC and HC alloys have densities of ~8.3 g/cm^3 and Young's moduli of ~220 GPa. The initial Vickers hardness, HV1, of the HC alloy is a little higher that of LC alloy as the strength hardening effect of carbide.

Fig. 2 shows the microstructure with equiaxed grains of ave. ~20 μm for (a) LC and (b) HC alloys, in which globular precipitates were observed predominantly precipitating along the grain